

# Calculation of penetration probability across an arbitrary potential barrier in fusion reactions

Yujiao Qin,<sup>1</sup> Junlong Tian,<sup>2</sup> Yongxu Yang,<sup>1</sup> and Ning Wang<sup>1,\*</sup>

<sup>1</sup>*Department of Physics, Guangxi Normal University, Guilin 541004, People's Republic of China*

<sup>2</sup>*School of Physics and Electrical Engineering, Anyang Normal University, Anyang 455002, People's Republic of China*

(Received 21 March 2012; revised manuscript received 10 May 2012; published 31 May 2012)

The penetration probability across an arbitrary nucleus-nucleus potential barrier is studied by using transfer matrix approach, including continuous variations of effective mass. The calculated penetration probabilities for reaction  $^{16}\text{O} + ^{208}\text{Pb}$  are closed to those of WKB and modified Numerov calculations based on the Bass potential. With the transfer matrix approach, the influence of the effective mass on the penetration probability are simultaneously investigated. The calculations imply that the effective mass is an important quantity for studying the hindrance of fusion cross sections of some reactions at deep sub-barrier energies. The fusion cross sections of heavy-ion fusion reactions and the resonance phenomena due to double-hump barriers are also studied with this approach.

DOI: [10.1103/PhysRevC.85.054623](https://doi.org/10.1103/PhysRevC.85.054623)

PACS number(s): 25.70.Jj, 23.60.+e, 27.90.+b

## I. INTRODUCTION

Quantum tunneling in microscopic systems is one of the fundamental phenomena in physics and chemistry. As an example, the tunneling plays a key role for fusion of two nuclei and  $\alpha$ -decay of heavy nuclei in nuclear physics at sub-barrier energies. In recent decades, heavy-ion fusion reactions have been extensively studied for synthesizing super-heavy elements [1–3] and for understanding the  $S$  factors [4–7] at deep sub-barrier energies in fusion reactions. Accurate calculation of the penetration probability across an arbitrary nucleus-nucleus potential barrier is of great importance for the description of the fusion cross sections and the  $\alpha$ -decay half-lives of super-heavy nuclei [8,9]. Therefore, a lot of methods for calculation of the penetration probability were proposed. One of the methods is to solve the Schrödinger's equations through the potential barriers such as the widely used code CCFULL [10], which applies the modified Numerov method for the coupled-channels calculations in the study of heavy-ion fusion reactions. The WKB (Wentzel-Kramers-Brillouin) approximation is also widely used for the quantum tunneling calculations. The traditional WKB method is inaccurate in regions where the potential profile varies abruptly [11], fails to describe the resonance phenomena, and encounters difficulty when the incident energies are close to the barriers. In addition, the effective mass (or mass parameter)  $\mu(R)$  was simply taken to be the reduced mass in many studies, such as in the modified Numerov calculations [10]. For fusion reactions of heavy nuclei, the process for penetrating the barrier becomes more complicated and the  $\mu(R)$  could not be simply taken to be the reduced mass [12,13]. Thus, the impact of the effective mass on the penetration probability should be studied. In this work, we attempt to calculate the penetration probability across an arbitrary potential barrier with an arbitrary incident energies based on the transfer matrix approach [11], including continuous variations of the effective mass.

This paper is organized as follows: In Sec. II, the transfer matrix method is introduced for calculation of the penetration

probability. In Sec. III, some calculated results with the transfer matrix approach based on some different nucleus-nucleus potentials are presented and compared with those from the WKB formula and the modified Numerov method. Finally, the conclusion is given in Sec. IV.

## II. TRANSFER MATRIX METHOD

In this section, for the reader's convenience, we first briefly introduce the WKB formula. Then we will introduce the transfer matrix method in detail. More introductions and calculations of the transfer matrix method were presented in Ref. [11]. For an arbitrary potential  $V(R)$  (as an example, the Bass potential [14] for the reaction  $^{16}\text{O} + ^{208}\text{Pb}$  is shown in Fig. 1), which is a function of distance  $R$  between two nuclei, the penetration probability across the potential barrier is expressed as

$$T = \exp \left\{ -\frac{2}{\hbar} \int_b^a \sqrt{2\mu(R)[V(R) - E]} dR \right\}, \quad (1)$$

according to the WKB approximation in a textbook. Where,  $\mu(R)$  is the coordinate dependent effective mass of the reaction system,  $\hbar$  is the reduced Planck constant, and  $E$  is the center-of-mass energy.  $a$  and  $b$  with  $V(R = a) = V(R = b) = E$  denote the classical turning points outside and inside of the barrier, respectively. From Eq. (1), one notes that the incident energy  $E$  can not be higher than the barrier height when applying this formula.

To describe the penetration probability at an arbitrary incident energy, we apply the transfer matrix approach, which is a method for accurately calculating the transfer coefficient across arbitrary potential barriers. In this method, the potential energy and the effective mass are approximately described by multistep functions (multistep potential approximation). In other words, the potential barrier is split into many segments, in which potential energy can be regarded as a constant. In the limit as the divisions become finer and finer, a continuous variation for the potential will be recovered.

\* wangning@gxnu.edu.cn

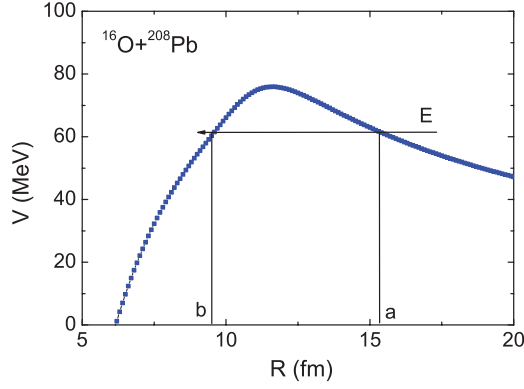


FIG. 1. (Color online) Bass potential for the reaction  $^{16}\text{O} + ^{208}\text{Pb}$ .

Assuming that the potential barrier is split into  $N$  small segments. An example, in the case where  $N = 9$ , is shown in Fig. 2, where the potential barrier  $V(R)$  and the effective mass  $\mu(R)$  are approximated by the multistep functions,

$$V_j = V\left(\frac{R_{j-1} + R_j}{2}\right) \quad (2)$$

$$M_l = \frac{1}{2} \begin{Bmatrix} (1 + S_l) \exp[-i(k_{l+1} - k_l)R_l] & (1 - S_l) \exp[-i(k_{l+1} + k_l)R_l] \\ (1 - S_l) \exp[i(k_{l+1} + k_l)R_l] & (1 + S_l) \exp[i(k_{l+1} - k_l)R_l] \end{Bmatrix} \quad (6)$$

and

$$S_l = \frac{\mu_{l+1}}{\mu_l} \frac{k_l}{k_{l+1}}. \quad (7)$$

By imposing the incoming wave boundary condition [10] (i.e., there are only incoming waves at  $R < R_N$  and the entrance channel has an incoming wave with amplitude one), one sets  $A_0 = 1$  and  $B_{N+1} = 0$  in Eq. (5) for  $j = N + 1$ , we can calculate the transfer amplitude  $A_{N+1}$  and the penetration probability  $T(E)$  as follows:

$$A_{N+1} = \frac{\mu_{N+1}}{\mu_0} \frac{k_0}{k_{N+1}} \frac{1}{M_{22}} \quad (8)$$

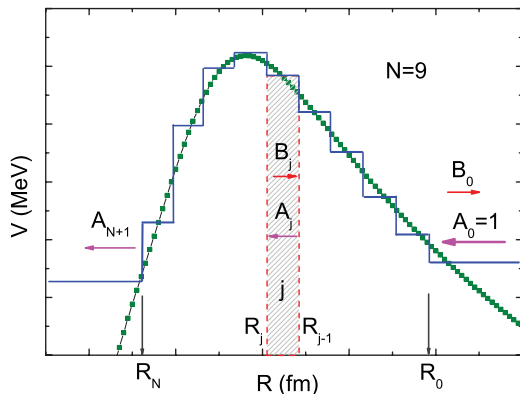


FIG. 2. (Color online) Bass potential (solid squares) and approximated potential function (multistep line) for the potential barrier.

and

$$\mu_j = \mu\left(\frac{R_{j-1} + R_j}{2}\right), \quad (3)$$

for  $R_{j-1} > R > R_j$  ( $j = 0, 1, 2, \dots, N, N + 1$ ). The wave function  $\psi_j(R)$  in the  $j$ th region, which is a combination of the incoming and outgoing waves and associated with the center-of-mass energy  $E$ , is given by

$$\psi_j = A_j \exp^{ik_j x} + B_j \exp^{-ik_j x}, \quad (4)$$

where  $k_j = \sqrt{2\mu_j(E - V_j)}/\hbar$ . From the continuity of the wave function and its derivative at each boundary, the determining of  $A_j$  and  $B_j$  in Eq. (4) can be reduced to the multiplication of the following  $N + 1$  ( $2 \times 2$ ) matrices:

$$\begin{pmatrix} A_j \\ B_j \end{pmatrix} = \prod_{l=0}^{j-1} M_l \begin{pmatrix} A_0 \\ B_0 \end{pmatrix}, \quad (5)$$

where

and

$$T(E) = \frac{\mu_0}{\mu_{N+1}} \frac{k_{N+1}}{k_0} |A_{N+1}|^2, \quad (9)$$

where

$$M = \begin{pmatrix} M_{11} & M_{12} \\ M_{21} & M_{22} \end{pmatrix} = \prod_{l=0}^N M_l. \quad (10)$$

### III. RESULTS

In this section, we first test the transfer matrix approach. Then we will study the influence of effective mass and double-hump shape of a nucleus-nucleus potential on the penetration probability.

Bass [14] derived a nucleus-nucleus potential using a geometric interpretation of fusion data above the barrier for fusion systems:

$$V_{\text{Bass}}(R) = -\frac{R_p R_t}{R_p + R_t} [0.033 \exp(s/3.5) + 0.007 \exp(s/0.65)]^{-1} + \frac{Z_p Z_t e^2}{R}, \quad (11)$$

where  $s = R - R_p - R_t$  denotes the separation between the half-density surfaces of the (spherical) interacting nuclei. The radius of the projectile nucleus  $R_p$  and that of the target  $R_t$  are derived by using  $R_{p,t} = R_s(1 - 0.98/R_s^2)$ , where  $R_s = 1.28A^{1/3} - 0.76 + 0.8A^{-1/3}$ .

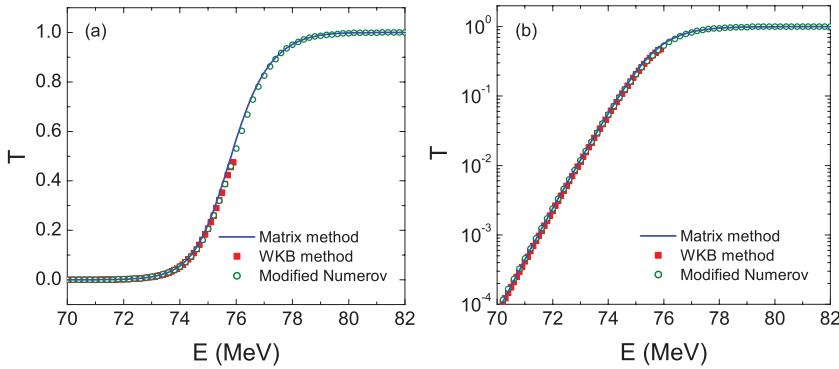


FIG. 3. (Color online) (a) Penetration probability based on the Bass potential for  $^{16}\text{O} + ^{208}\text{Pb}$ . The solid curve, squares, and open circles denote the results with the transfer matrix approach, the WKB formula and the modified Numerov method, respectively. (b) The same as (a) but in the logarithmic scale.

Figure 3 shows the obtained penetration probability based on the Bass potential in Fig. 1 with the transfer matrix approach (solid curve), the WKB formula (squares), and the modified Numerov method (open circles), respectively. The modified Numerov method adopted in the CCFULL code solves the Schrödinger's equations outwards from the minimum position of the Coulomb pocket by imposing the incoming wave boundary condition mentioned previously. When the incident energies are below the Coulomb barrier, the results from these three different approaches are close to each other. At energies above the Coulomb barrier, the results from the modified Numerov and those with the transfer matrix method are also close to each other. The variation of the effective mass  $\mu$  in fusion process has not yet been considered in the present version of CCFULL code [10]. We therefore temporarily set the effective mass to be the reduced mass  $\mu_0 = \frac{A_p A_t}{A_p + A_t} m$  with the nucleon mass  $m$  in this calculation for comparison.

With the transfer matrix method, the influence of the variation of the effective mass on the penetration probability

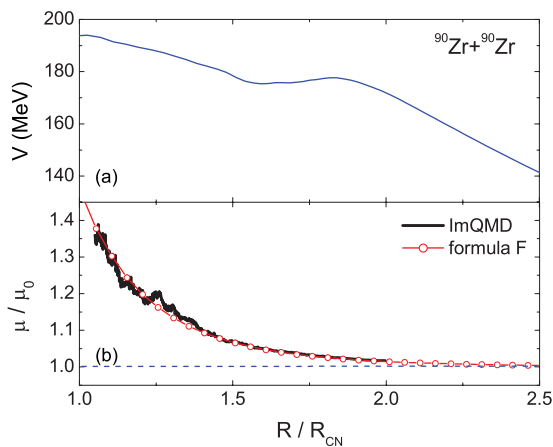


FIG. 4. (Color online) (a) Nucleus-nucleus potential of  $^{90}\text{Zr} + ^{90}\text{Zr}$  by using the ImQMD model with the parameter set IQ2 and the incident energy of  $E = 200$  MeV. (b) Effective mass  $\mu$  as a function of center-to-center distance  $R$ . Here,  $\mu_0 = \frac{A_p A_t}{A_p + A_t} m$  denotes the reduced mass of the reaction system.  $R_{\text{CN}} = 1.16(A_p + A_t)^{1/3}$  denotes the radius of the compound nucleus. The thick solid curve denotes the results of the ImQMD simulations with IQ2 in Ref. [12]. The open circles denote an empirical formula  $F(R) = 1 + \exp(-0.72R/R_{\text{CN}})(R/R_{\text{CN}})^{-4}$  with the parameter by fitting the solid curve.

can be simultaneously studied. In Ref. [12], the mass parameter for the relative motion in heavy-ion fusion reaction  $^{90}\text{Zr} + ^{90}\text{Zr}$  was studied with the improved quantum molecular dynamics (ImQMD) model [15], and it is found that the effective mass  $\mu$  is around the reduced mass  $\mu_0$  when the reaction partners are at the separated configuration and increases with a decrease of the distance between two reaction partners after the touching configuration. With the ImQMD model and the same approach as was used in Ref. [16], the dynamical nucleus-nucleus potential of  $^{90}\text{Zr} + ^{90}\text{Zr}$  is calculated and shown in Fig. 4(a). To calculate the penetration probability more conveniently, we describe the variation of the effective mass  $\mu(R)$  by using an empirical formula  $F(R) = 1 + \exp(-0.72R/R_{\text{CN}})(R/R_{\text{CN}})^{-4}$ , i.e.,  $\mu(R) = \mu_0 F(R)$  for this reaction. From Fig. 4(b), one sees that the formula  $F(R)$  reproduces the ImQMD calculations reasonably well. Figure 5 shows the comparison of the calculated penetration probability by using the transfer matrix method for the cases with the effective mass  $\mu = \mu_0$  and  $\mu = \mu_0 F$ , respectively. When the incident energies are below the Coulomb barrier, the penetration probabilities strongly depend on the effective mass adopted. The penetration probability is significantly reduced with the increasing of the effective mass at short distances comparing with the case taking  $\mu = \mu_0$ . These investigations indicate that the effective mass should also be considered for explaining the hindrance of fusion cross sections of some

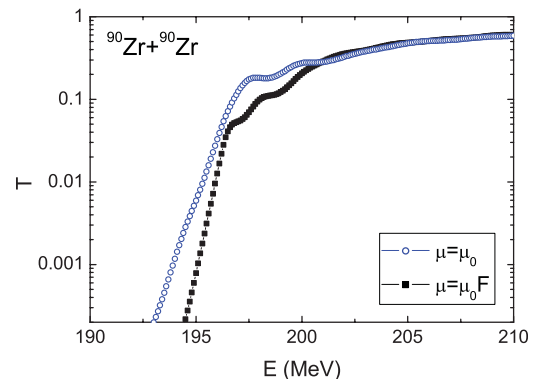


FIG. 5. (Color online) Penetration probability across the potential barrier in Fig. 4(a) by using the transfer matrix method for the cases with the effective mass  $\mu = \mu_0$  (open circles) and  $\mu = F\mu_0$  (solid squares), respectively. Here, we set  $R_N = 5$  fm in the calculations.

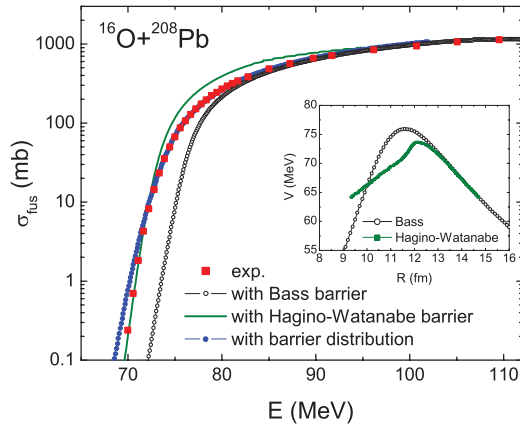


FIG. 6. (Color online) Fusion excitation function of  $^{16}\text{O} + ^{208}\text{Pb}$ . The solid curve and open circles denote the results with the Hagino-Watanabe potential and Bass potential, respectively. The squares and solid circles denote the experimental data taken from Ref. [18] and the results in Ref. [19] based on an empirical barrier distribution, respectively. The open circles and solid squares in the inset denote the Bass potential and the potential proposed by Hagino and Watanabe for  $^{16}\text{O} + ^{208}\text{Pb}$ , respectively.

reactions at deep sub-barrier energies, in addition to the nuclear potentials.

With the transfer matrix method and different nucleus-nucleus potentials of  $^{16}\text{O} + ^{208}\text{Pb}$ , the fusion cross sections for this reaction at energies around the Coulomb barrier are studied simultaneously. Here, the centrifugal potential  $\frac{l(l+1)\hbar^2}{2\mu R^2}$  is added to the nucleus-nucleus potential to consider the angular momentum  $l$  of the relative motion. With the penetration probability from the transfer matrix method, one can obtain the corresponding fusion cross section:

$$\sigma_{\text{fus}}(E) = \frac{\pi}{k_0^2} \sum_l (2l+1) T_l(E). \quad (12)$$

Figure 6 shows the calculated fusion excitation function of  $^{16}\text{O} + ^{208}\text{Pb}$ . The solid curve and open circles denote the results with the Hagino-Watanabe potential [17], which is extracted by inverting the experimental data for heavy-ion fusion reactions at energies well below the Coulomb barrier and the Bass potential, respectively. The squares and small solid circles denote the experimental data taken from Ref. [18] and the results in Ref. [19] based on an empirical barrier distribution, respectively. Here, we set  $\mu = \mu_0$  in the calculations of the fusion cross sections at energies around the Coulomb

barrier. (For fusion reaction at deep sub-barrier energies, one should consider the variations of the effective mass.) With the extracted barrier by Hagino and Watanabe, the fusion cross sections of  $^{16}\text{O} + ^{208}\text{Pb}$  at sub-barrier and over-barrier energies can be described reasonably well; however, the fusion cross sections at energies near the Coulomb barrier cannot be described well. With the Bass potential, the fusion cross sections at sub-barrier energies are under-predicted. It is known that the one-dimensional barrier penetration model with empirically determined potential barrier is successful in describing the fusion excitation functions for light systems. For heavy systems, the coupling of the relative motion to internal degrees of freedom which causes a barrier distribution should be taken into account. With the empirical barrier distribution and the barrier penetration concept, it was found that the experimental data can be reproduced well [19].

Finally, we investigate the resonance phenomena in fusion reactions between light nuclei such as  $^{12}\text{C} + ^{12}\text{C}$  [20]. The resonance phenomena due to the double-hump fission barriers of some actinide nuclei is also found in fission process. To check the transfer matrix approach for describing the resonance phenomena, we construct some potentials based on the Bass potential, by introducing an inner barrier of Gaussian form inside the Coulomb barrier,

$$V = V_{\text{Bass}} + C \exp\left[-\frac{(R-3)^2}{2}\right], \quad (13)$$

with the parameter  $C$  to adjust the height of the inner barrier. Figure 7 shows the constructed potential barriers with different values of  $C$  and the corresponding penetration probability obtained with the transfer matrix approach. With increasing the value of  $C$ , the height of the inner barrier increases. We note that there exists obvious resonance peak for the penetration probability when the inner barrier height is comparable to the outer barrier height. The resonance due to the quantum effect can result in a significant change of the penetration probability at a certain incident energy.

#### IV. SUMMARY

The penetration probability across an arbitrary potential barrier has been investigated by using the transfer matrix approach. The calculated penetration probability across the Bass barrier is close to the results of the WKB formula and those of modified Numerov method. By using the transfer matrix method, various potential barriers and wells can be

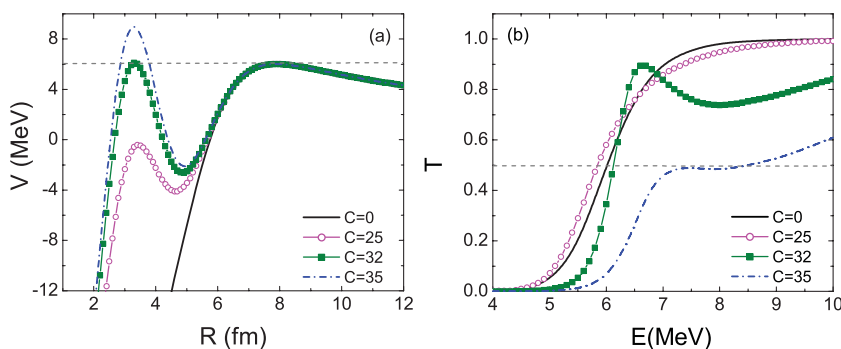


FIG. 7. (Color online) (a) Modified Bass potential barriers with different values of  $C$ . (b) Corresponding penetration probability across the potential barriers in (a). The short-dashed lines are to guide the eyes.

analyzed, including continuous variations of the effective mass, which is not considered in commonly used numerical schemes such as the modified Numerov method adopted in the CCFULL code. The penetration probability is significantly reduced at energies below the potential barrier with the increasing of the effective mass at short distances comparing with the case taking the reduced mass, which indicates the effective mass is an important quantity for studying the hindrance of fusion cross sections of some reactions at deep sub-barrier energies. With the transfer matrix method and different nucleus-nucleus potentials of  $^{16}\text{O} + ^{208}\text{Pb}$ , the corresponding fusion cross sections at energies around the Coulomb barrier have been studied simultaneously. We find that for heavy systems, the coupling of the relative motion to internal degrees of freedom which causes a barrier distribution should be taken into account for a reasonable description

of the fusion cross sections spanning the Coulomb barrier. The resonance phenomena can be clearly observed for some double-hump barriers, especially when the inner barrier height is close to the outer barrier height. The resonance due to the quantum effect can result in a significant change of the penetration probability at a certain incident energy. These investigations are helpful for understanding the mechanism of fusion reactions at deep sub-barrier energies and the resonance phenomena.

#### ACKNOWLEDGMENTS

We thank the anonymous referee for valuable suggestions. This work was supported by National Natural Science Foundation of China, Grants No. 10875031, No. 11005003, No. 10865002, No. 10979024, and No. 10847004.

- 
- [1] A. Sobczewski and K. Pomorski, *Prog. Part. Nucl. Phys.* **58**, 292 (2007).
  - [2] Yu. Ts. Oganessian *et al.*, *Phys. Rev. Lett.* **104**, 142502 (2010).
  - [3] N. Wang, J. Tian, and W. Scheid, *Phys. Rev. C* **84**, 061601(R) (2011).
  - [4] C. L. Jiang *et al.*, *Phys. Lett. B* **640**, 18 (2006).
  - [5] Ş. Mişicu and Florin Carstoiu, *Phys. Rev. C* **84**, 051601(R) (2011).
  - [6] H. Q. Zhang, C. J. Lin, F. Yang *et al.*, *Phys. Rev. C* **82**, 054609 (2010).
  - [7] Ş. Mişicu and H. Esbensen, *Phys. Rev. Lett.* **96**, 112701 (2006).
  - [8] C. Xu and Z. Ren, *Nucl. Phys. A* **753**, 174 (2005).
  - [9] H. F. Zhang, Y. Gao, N. Wang, J. Q. Li, E. G. Zhao, and G. Royer, *Phys. Rev. C* **85**, 014325 (2012).
  - [10] K. Hagino, N. Rowley, and A. T. Kruppa, *Comp. Phys. Comm.* **123**, 143 (1999).
  - [11] Y. J. Ando and T. H. Ioth, *J. Appl. Phys.* **61**, 4 (1987).
  - [12] K. Zhao, Z. Li, X. Wu, and Z. Zhao, *Phys. Rev. C* **79**, 024614 (2009).
  - [13] T. Ichikawa, K. Hagino, and A. Iwamoto, *Phys. Rev. C* **75**, 057603 (2007).
  - [14] R. Bass, *Lecture Notes in Physics* 117 (Springer, Berlin, 1980), pp. 281–293.
  - [15] N. Wang, Z. Li, X. Wu, J. Tian, Y. X. Zhang, and M. Liu, *Phys. Rev. C* **69**, 034608 (2004).
  - [16] Y. Jiang, N. Wang, Z. Li, and W. Scheid, *Phys. Rev. C* **81**, 044602 (2010).
  - [17] K. Hagino and Y. Watanabe, *Phys. Rev. C* **76**, 021601(R) (2007).
  - [18] C. R. Morton, A. C. Berriman, M. Dasgupta, D. J. Hinde, J. O. Newton, K. Hagino, and I. J. Thompson, *Phys. Rev. C* **60**, 044608 (1999).
  - [19] M. Liu, N. Wang, Z. Li, X. Wu, and E. Zhao, *Nucl. Phys. A* **768**, 80 (2006).
  - [20] B. Sahu, S. K. Agarwalla, and C. S. Shastri, *Pramana-J. Phys.* **61**, 51 (2003).